The cardiac, respiratory, and gastric rhythms independently modulate motor corticospinal excitability in humans

Tahnée Engelen[1,2]*, Teresa Schuhmann[3], Alexander T. Sack[3], Catherine Tallon-Baudry[1]*

Corresponding authors*:

tahnee.engelen@yahoo.nl

catherine.tallon-baudry@ens.psl.eu

Affiliations:

1. Cognitive and Computational Neuroscience Laboratory (LNC2), INSERM U960, Department of Cognitive Studies, Ecole Normale Supérieure, PSL University, 29 rue d'Ulm, 75005 Paris, France
2. Department of Psychology, Faculty of Education and Psychology, University of Jyväskylä, P.O. Box 35, FI-40014, Jyväskylä, Finland
3. Section Brain Stimulation and Cognition, Department of Cognitive Neuroscience, Faculty of Psychology and Neuroscience, Maastricht University, P.O. Box 616, 6200 MD, Maastricht, The Netherlands

Keywords:

Interoception, visceral rhythms, brain-body interactions, corticospinal excitability

Abstract

Interoception refers to the brain's sensing of internal body state and encompasses various bodily systems, notably the cardiac, respiratory and gastric rhythms. Beyond their roles in physiological regulation and emotional states, each of these visceral rhythms has been shown to influence brain activity and cognition, prompting for the development of various interpretative functional frameworks. However, both experimental data and functional hypothesis leave it unclear whether and how each visceral rhythm acts simultaneously and independently on brain activity. Here we address this question by measuring in human participants how the corticospinal excitability of the motor system varies with the phase of each of the three visceral rhythms. We applied single pulse Transcranial Magnetic Stimulation (TMS) over the hand region in primary motor cortex to elicit Motor Evoked Potentials (MEP), whose amplitude reflects corticospinal excitability, and tested whether MEP amplitude depends on the phase of the simultaneously measured cardiac, respiratory and gastric rhythms. All three visceral rhythms contributed to motor excitability with similar effect sizes at the group level. However, we found no relation between coupling strengths: participants

displaying high coupling with one organ did not necessarily display high coupling to the other organs. These results indicate that independent mechanisms underly the coupling between the cardiac, respiratory and gastric rhythm and motor excitability. We further introduce the concept of individual interoceptive profiles, and show that such interoceptive profiles obtained from objective coupling strength measures were not explained by self-reported awareness of the organ. Altogether our results call for refined specifications of the frameworks offering a functional or clinical interpretation of viscera-brain coupling taking into account both independent mechanisms and individual interoceptive profiles.

1. Introduction

Interoception refers to the sensing of internal bodily signals, for which signals from the heart, lungs and stomach are considered core components, both in the original definition by Sherrington (1) and in more recent views (2,3). The function of interoception is obviously associated with homeostatic regulations, and as such is involved in responses to physiological challenges or emotional contexts. However, experimental evidence suggests a functional role for interoception beyond physiological regulation. In perceptual and cognitive tasks that have no apparent link to homeostatic constraints and are emotionally neutral, a growing number of experimental studies find coupling between a visceral rhythm and brain activity and/or reaction times (4,5). Such findings have motivated a number of theoretical proposals hypothesising on the functional role of the interaction between interoception and the cognitive brain and behaviour.

Some proposals focus specifically on action, such as active sensing, i.e. the notion that sensing external information is an active process involving motor sampling (6). Respiration plays a key active sensing role for olfaction, because inhalation is required for odour detection (7). By extension, experimental findings involving other sensory modalities and other visceral rhythms have been interpreted in the active sensing framework, for instance the over-abundance of saccades to explore the visual environment in the early phase of the cardiac cycle (8,9). Other functional proposals are even more general. For instance, visceral rhythms could provide a temporal scaffold to facilitate large-scale neuronal coordination, with experiments on the coupling of respiration and limbic regions in rodents (10,11) or on the coupling between the slow gastric rhythms and all sensory and motor cortices in humans (12,13) interpreted along those lines. Both lines of thinking are appealing and not necessarily mutually exclusive. The point we want to raise here is that such frameworks are applied relatively indiscriminately to any visceral rhythm. In other words, there is an unformulated underlying assumption that although the cardiac, respiratory and gastric rhythms support distinct physiological functions and operate at markedly distinct dominant frequencies (in humans respectively, 1Hz, 0.2 Hz and 0.05Hz) (for review, see 5), they can nevertheless fit within the same interpretative framework. Still, no experiment to date measured all three visceral rhythms: the vast majority of experiments are limited to one visceral rhythms, with few notable exceptions combining two (14–16).

Here, as a first attempt to bridge the gap between generic interpretative frameworks and rhythm-specific experimental data, we ask whether the excitability of the motor system is simultaneously and independently modulated by the cardiac, respiratory and gastric rhythms.

The motor system is a good candidate since movement onsets (8,9,17–19), response inhibition (20,21), discharge of alpha motoneurons (22), and motor cortico-spinal excitability (23) vary along the cardiac cycle. The phase of respiration affects the timing of voluntary (15,24) and involuntary (25) actions, motor-related neural activity (15,26), and changes in breathing style influence motor cortico-spinal excitability (27,28). Finally the gastric rhythm is consistently coupled to motor and premotor areas at rest in humans (12,13) as well as in anaesthetized rodents (29,30). In practice (Figure 1), we probed non-invasively corticospinal excitability in human male and female participants by measuring from a hand muscle the motor evoked potentials (MEPs) induced by Transcranial Magnetic Stimulation (TMS) over primary motor cortex (31,32). MEPs typically measure excitability from primary motor cortex down to the final muscle where they are measured, including spinal relays (32). We tested for relationships between MEPs and the phase of the simultaneously recorded cardiac, respiratory and gastric rhythms.

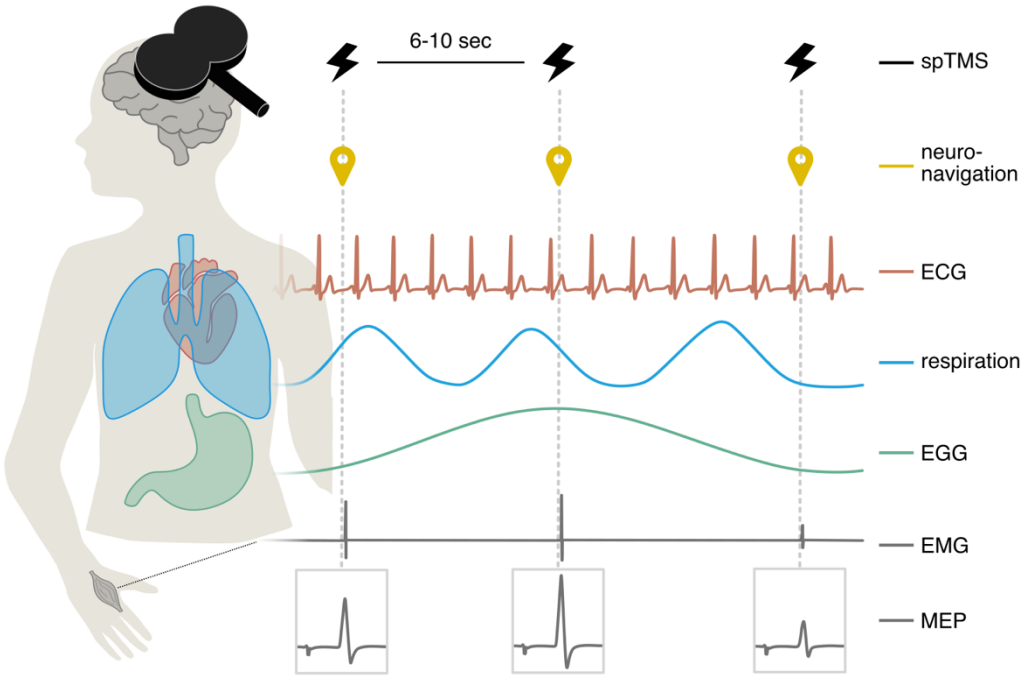

Figure 1. Experimental set up. Single pulses of TMS were applied to the hand area of the right primary motor cortex with an inter-pulse interval randomized between 6 and 10 seconds. Simultaneously, the neuronavigated coil position (yellow), electrocardiogram (red), respiratory signal (blue), electrogastrogram (green) and electromyography from the left hand (gray) were recorded. The experimental measure was the Motor Evoked Potential amplitude measured on a hand muscle (first dorsal interosseous), analysed against the phase of the cardiac, respiratory and gastric rhythms. Note that the three rhythms have very different periods (~1s for the heart, ~5 s for respiration, and ~20s for the gastric rhythm). Abbreviations: spTMS, single pulse transcranial magnetic stimulation; ECG, electrocardiogram; EGG, electrogastrogram; EMG, electromyogram; MEP: motor evoked potential.

2. Materials & Methods

2.1 Participants

29 healthy participants completed the experiment after providing written informed consent. The study was approved by the Ethics Review Committee Psychology and Neuroscience of Maastricht University (reference number ERCPN-247_01_01_2022). Participants received a voucher reward of 10 euros per hour. Inclusion criteria were to be aged above 18 years and to have a Body Mass Index (BMI) lower than 25 to ensure good quality gastric recordings (33). Participants were further screened for MRI and TMS safety. One participant was excluded from analysis due to issues with recording of the respiration signal. In total, 28 participants were included in the final analysis (8 male, 2 left handed, mean age(SD) = 27.36(8.98), mean BMI(SD) = 21.76(2.38)).

2.2 Experimental procedure, general organization

The experiment consisted of two sessions. During the first session an anatomical MRI scan was acquired at rest. At the start of the second session participants completed the questionnaires, after which all physiological recordings were prepared and TMS intensity and stimulation site were determined. Participants completed three blocks of the task, each lasting around 16 minutes, while the TMS stimulation was applied. Participants were in a seated position with their head supported by a chin rest, were instructed to fixate on a screen and were given a task to avoid drowsiness (see 2.5 for task details).

2.3 TMS application and neuronavigation recordings

Single pulse TMS was applied over right M1 hotspot using a MC-B70 figure-of-eight coil and Magpro X100 stimulator (MagVenture A/S, Farum, Denmark). Participants were co-registered to their individual anatomical T1 MRI (TR = 2300 ms, TE = 2.98 ms, TI = 900 ms, 192 slices, FOV = 256 mm, matrix sixe = 256 × 256, 1 mm isotropic voxel, acquired on 3T Siemens Prisma Fit) and coil position was recorded throughout the session using a neuronavigation system (Localite GmbH, Bonn, Germany). The coil was placed tangentially to the scalp with the handle pointing backward at a 45-degree angle from the midline. Individual stimulation intensity was set to elicit an MEP of approximately 1mV in amplitude (mean stimulation intensity(SD) = 41(7)% maximum stimulator output). The stimulation target was identified by applying single pulses over the right hemisphere until the location showing a maximum response from the left first dorsal interosseous muscle (FDI) was found, which was set as the target for the rest of the session. The interpulse interval was jittered between six and ten seconds and a total of 360 pulses were applied during the task, subdivided into three blocks. The difference between coil and target location was calculated off-line as follows:

$$\text{Coil distance} = \sqrt{(dP^2 + dS^2 + dL^2)}$$

where *dP*, *dS*, and *dL* are the difference between location of the coil and the set target in the Posterior, Superior, and Lateral dimensions. Trials on which the coil distance exceeded more than four standard deviations from the mean of the participant were excluded from analysis.

2.4 Physiological recordings

Physiological signals were recorded using a BrainAmp ExG amplifier and the BrainVision Recorder software (Brain Products GmbH, Gilching, Germany) at a 5000Hz sampling rate. All signals were recorded with a high cut-off of 1000Hz and with a low cut-off filter set to a time constant of 10 seconds for electromyography (EMG) and the electrocardiogram (ECG) and DC for respiration and the electrogastrogram (EGG). A respiration belt containing a pneumatic pressure-sensitive cushion was placed around the chest to record thoracic respiratory movements. All other signals were recorded with bipolar montage using cutaneous AgCl ring electrodes. Motor evoked responses were recorded using EMG of the left FDI muscle following the belly-tendon montage with one electrode placed over the belly of the muscle and a reference electrode placed along the outside of the index finger. The ECG was recorded by placing one electrode below the right clavicle and the other electrode on the left lower abdomen (lead II). The EGG was recorded using a grid of six electrodes on the left side of the belly, all referenced to an electrode on the upper right side of the belly, following recommendations of Wolpert et al. (2020).

2.5 Task and eyetracking

To help participants remaining wakeful during data acquisition, one quadrant of the black circle surrounding the fixation point could occasionally turn white for 500ms. In each block 16 targets were randomly presented, always starting/ending with at least 500ms distance to the TMS pulse. To avoid contamination of manual motor actions on MEP amplitude, participants responded by making an eye movement to the corner of the screen in the direction at which the target appeared. Eye position was tracked using an Eyelink 1000 system (SR Research, Canada), using a monocular recording of the right eye with a 16mm lens at a sampling rate of 1000 Hz.

2.6 Questionnaires

To measure self-reported interoception, participants completed two questionnaires prior to the start of the experiment, the Three-domain Interoceptive Sensations Questionnaire (THISQ)

(34) and the Multidimensional Assessment of Interoceptive Awareness, Version 2 (MAIA-2) (35).

2.7 Data pre-processing

Offline pre-processing and analysis of physiological signals was done using the Fieldtrip toolbox implemented in Matlab (Matlab version 2024a and Fieldtrip version 20220104) (36) and additional custom-built Matlab code. Continuous EMG data was band-pass filtered between 1 and 1000Hz using a 4th order forward and backward Butterworth filter and segmented around the TMS pulse (-1 to +1 second). MEP amplitude was calculated as the difference between the local maximum and local minimum between 20-60ms after the pulse. MEPs were excluded if their amplitude was below 50μV, their amplitude got cut off due to amplifier saturation, their amplitude exceeded the mean of the participant by more than four standard deviations, or if the signal to noise ratio (SNR) between the time preceding the pulse relative to the MEP amplitude was below three. SNR was calculated as the amplitude of the MEP divided by the maximum RMS value in the 500-10ms preceding the pulse.

Continuous ECG data was band-pass filtered between 1 and 40 Hz (windowed-sinc FIR filter, onepass-zero phase shift). A participant and block specific template heartbeat was computed and convolved with the ECG time series. R-peaks were identified on the normalized convolution as exceeding a threshold of 0.6. Misidentified R-peaks were manually corrected. Further cardiac events were defined relative to the R-peak as local minima or maxima in preset time windows. For the T-wave this was a local maximum occurring within 420ms after the Q-wave. Noisy cycles were identified by excluding any cycles in which the RT interval exceeded three standard deviations from the mean of that block. Instantaneous cardiac phase was calculated by assigning radian values between 0 and 2π to each TMS pulse based on its relative timing within the RR interval. To further characterize systole and diastole, we determined the end of the T-wave. A block-by-block mean T wave was computed, and the local maximum in the second derivative of this signal in between the peak of T up to + 150ms was found. The mean end of T time between the three blocks was used to define cardiac systole (R peak to end of T) and cardiac diastole (end of T to next R).

Continuous respiration data was smoothed using a 750ms window moving average (Matlab movmean). Expiration onset was identified on the z-scored respiration signal using the findpeaks function with a minimum peak distance of 1 seconds and minimum peak prominence set to the mean positive peak height excluding extreme values (peaks exceeding three times the standard deviations from the mean signal are excluded). The beginning of inspiration was

determined by using an adapted version of the trapezoid area algorithm (37). Briefly, this involved iteratively fitting trapeziums on the derivative of the respiration signal, and finding the area where the trapezoid has the largest area, which is taken as inspiration onset. Artefacted segments were identified by manual inspection. Cycles with either inspiration or expiration length exceeding the mean length of inspiration and expiration of the respective block by four SDs were excluded from further analysis. Instantaneous respiratory phase was calculated by assigning radian values between 0 and 2π to each TMS pulse based on its relative timing to the start of inspiration and end of expiration interval.

EGG data was preprocessed following the steps described in Wolpert et al. (2020). Data was demeaned, detrended, and down-sampled to 1000Hz. A Fast-Fourier Transform (FFT) with a Hanning taper was used to identify the channel with the largest spectral activity in the normogastric range (0.033-0.067Hz), which was then selected for further analysis. Data was band-width filtered around individual peak frequency $\pm$0.015Hz using a third-order finite impulse responses filter (Matlab FIR2). Artefacted segments were identified as cycles whose length exceeded three SDs from the mean cycle length (except two participants where SD criterion of two was used due to noisier data) or which displayed nonmonotonic changes in phase. Instantaneous phase was retrieved by Hilbert transforming the filtered data.

After preprocessing, a mean(SD) of 287(41) out of 360 trials per participant remained for analysis (min: 191 ; max: 342).

2.8 Statistical analysis

2.8.1 General

General support for or against the null hypothesis was quantified using the Bayes Factor (BF) using formulas provided by Liang et al. (2008). BF_{10} values smaller than 0.33 indicate moderate support for H_0, and values smaller than 0.1 indicate strong evidence for H_0. On the other end, values exceeding 3 indicate support for H_1, and values exceeding 10 indicate strong evidence for H_1. Reported effect sizes are quantified using Hedge's g (Matlab meanEffectSize), where effects above 0.2 are considered small, 0.5 considered medium, and 0.8 considered large. Reported correlations are calculated based on a ranked correlation test (Kendall's tau B implemented in JASP (JASP Team (2024)) and a False Discovery Rate (FDR) correction of p-values is applied if necessary. The pre-specified alpha for all reported statistics is set to 0.05.

2.8.2 The effect of coil distance on MEP amplitude

To account for the effect of displacement of the TMS coil with respect to the participant's head, we modelled the influence of coil distance on the MEP amplitude. This is particularly relevant given that head displacement caused by the participant's respiratory rhythm could potentially explain phase locked amplitude changes. We modelled the trial-by-trial z-scored peak to peak amplitude of the MEP with the z-scored coil distance value for each participant separately using a general linear model (GLM) in the following manner:

GLM Model 1:

$$[z(MEP_{amplitude})] \sim \beta_0 + \beta_{coil\ distance} * [z(\text{Coil distance})] + MEP_{residuals}$$

To test for significance, the beta values for the coil distance regressor were tested against zero using a two-tailed paired t-test. Given the significant result of this analysis, all subsequently described analyses are performed on the residuals resulting from this model. In other words, our analyses of interest are performed on amplitude values which have been corrected for the effect of coil distance.

2.8.3 Assessing phase-amplitude coupling between visceral rhythms and MEPs

To test whether the amplitude of the MEP was coupled to the phase of either the cardiac, respiratory, or gastric rhythm (visceral phase with MEP amplitude coupling), we used a circular spline generalized circular model (39). This method allows for computing participant specific chance levels of phase-amplitude coupling, meaning it does not require phase-alignment on the group level, which is unlikely to be the case for the gastric rhythm where there is no true zero point in the cycle (33). Briefly, the circular GLM (normal distribution, identity link function) involves fitting two models, the spline model in which cardinal splines are fitted to each participant's data to estimate amplitude as a function of phase, and a null model. The spline model is fitted based on a number of control points which is estimated for each participant separately using the Akaike information criterion (mean(SD) control points for cardiac = 4.5(1.4), for respiration = 4.7(1.3), and gastric = 4.7(1.6)). In the null model each data point corresponds to the mean of the data, generating data with a uniform distribution along phase. To quantify phase-amplitude coupling the maximum absolute deviation between the spline and null model is calculated (r value). The larger the r value, the more the empirical data deviate from a uniform distribution. We ran one model *per visceral signal* (thus three models) and *per participant* to obtain individual empirical r values.

Importantly, large r-values could be obtained by chance. Thus, to further determine whether the significance of empirically obtained r values, we estimated the chance distribution of r

values for each participant. We ran the model described above 1000 times, each time shuffling the phase labels associated to each trial. A participant's coupling strength was then computed by subtracting the median of the permuted r value distribution from the empirical r value. Because circular spline GLMs allow for only one circular regressor, we thus tested each visceral rhythm separately. Statistical significance of coupling strengths at the group level was assessed with a one-sided Wilcoxon signed-rank test against zero. Importantly, the aim of this analysis is thus to test whether there is higher phase-amplitude coupling than chance level.

Lastly, we wanted to test for the inter- or independence of coupling of the different visceral rhythms to the motor system in another manner besides correlations between the coupling strengths, to ensure our findings are not simply a result of our chosen analysis technique. To this end we opted for a simple GLM, similar to the one used to estimate the effect of coil distance on MEP amplitude, in which all three visceral rhythms are entered as well as their interactions. To be able to analyse circular data, such as visceral phase, in a simple GLM required the binarization of the data. To this end, the visceral phases were split into one 'excitatory' and one 'inhibitory' phase based on each individual's data. As these windows of excitation and inhibition were based on individual data, they could thus differ between participants and were not necessarily linked to specific physiologically meaningful phases. The excitatory and inhibitory phase were established for each participant and each visceral rhythm as follows: data was divided into six equally spaced phase bins between 0 and 2pi. Excitatory phase was defined as the phase bin with the highest mean residual MEP values and the two adjacent bins, and inhibitory phase consisted of the three remaining bins.

This approach allowed us to add all three visceral rhythms and their interactions into the same model (rather than one model per signal), which was not possible in the circular spline model. The influence of binary visceral phase on the residual values was then estimated in the following way:

GLM Model 2:

$$MEP_{residuals} \sim \beta_0 + \beta_{cardiac\ phase} + \beta_{respiratory\ phase} + \beta_{gastric\ phase} + \beta_{cardiac\ *\ respiratory\ phase} + \beta_{respiratory\ *\ gastric\ phase} + \beta_{cardiac\ *\ gastric\ phase} + \beta_{cardiac\ *\ respiratory\ *\ gastric\ phase}$$

Importantly, this model did not aim to see if the phase of each visceral rhythm explains the MEP residuals, as this was already established with the spline models, and phase effects are here enforced by splitting the data based on optimal phase. Rather, the goal was to be able to investigate the interaction effects on the MEP residuals, as reveal whether the visceral phase effects previously observed are independent. To test for significance of the interaction

terms, the beta values of the interaction term regressors were tested against zero using a two-tailed paired t-test.

2.8.4 The relationship between visceral-motor coupling and self-reported interoception

We wanted to test for relationships between objective measures of brain-viscera coupling and the extent to which participants themselves indicate to be aware of their internal organs. To do so, we correlated each participants organ-specific coupling strength with the matching organ specific scores obtained in the THISQ questionnaire (e.g. cardiac coupling strength correlated with cardiac THISQ score). We also tested for a correlation between coupling strengths and a widely adopted interoception questionnaire, the MAIA-2 (35). For the correlation analysis we focused on the correlations between the coupling strengths and the body listening and noticing sub-scores, which refer to the awareness of bodily signals and active listening to the body for insight respectively, as they were closest to our research questions. Correlations with the MAIA questionnaires were FDR corrected for six tests (two sub-scores by three coupling strengths).

2.8.5 Inter-individual variability in the alignment to physiological phases

The circular spline GLM specifically tests whether there is phase-amplitude coupling between the visceral rhythms and corticospinal excitability, however it does not conclude anything about whether the exact optimal phase is consistent between participants. This means that one participant could have a strong increase in excitability early in the cardiac phase and another late in the cardiac phase. However, based on existing literature such increases in motor excitability might occur in specific moments in either the cardiac or respiratory cycle (e.g. Al et al., 2023; Park et al., 2020). To test for this possibility, we ran an exploratory analysis in which the data was divided into six equally spaced phase bins between zero and 2pi for each participant, and extracted their mean bin residual value, and which bin had the highest mean. We here specifically focused on the data wrapped to the physiologically meaningful phases, so bins between zero and pi represent either systole or inspiration, and between pi and 2pi represent either diastole or expiration. This analysis allows looking at whether group mean bin values show patterns across the cycle, and whether the highest bin is consistent on the group level. Note that here we do not further examine the gastric rhythm, as the exact starting point of each cycle is unknown and thus looking at group level consistency is not meaningful.

3. Results

3.1 Coil distance-to-target explains MEP amplitude

The distance of the TMS coil to the target stimulation site in the motor cortex is known to influence MEP amplitude (40). This distance also varies with experimenter and/or participant movement and might thus be in particular related to the participant's breathing movement, which would confound all further analysis. Our first step was to quantify the influence of coil distance-to-target on MEP amplitude (GLM model 1). As expected from the literature ((40,41)), smaller distance of the coil to the target resulted in larger MEP amplitudes (paired -t-test against 0, $t(27) = -5.26$, $p < 0.001$), with a BF_{10} of 1475 indicating strong support for the alternative hypothesis, and a Hedge's g of -0.97 indicating a large effect (see figure 2A). All subsequent analyses are performed on MEP fluctuations unrelated to coil distance-to-target fluctuations, i.e., the residuals of this first model.

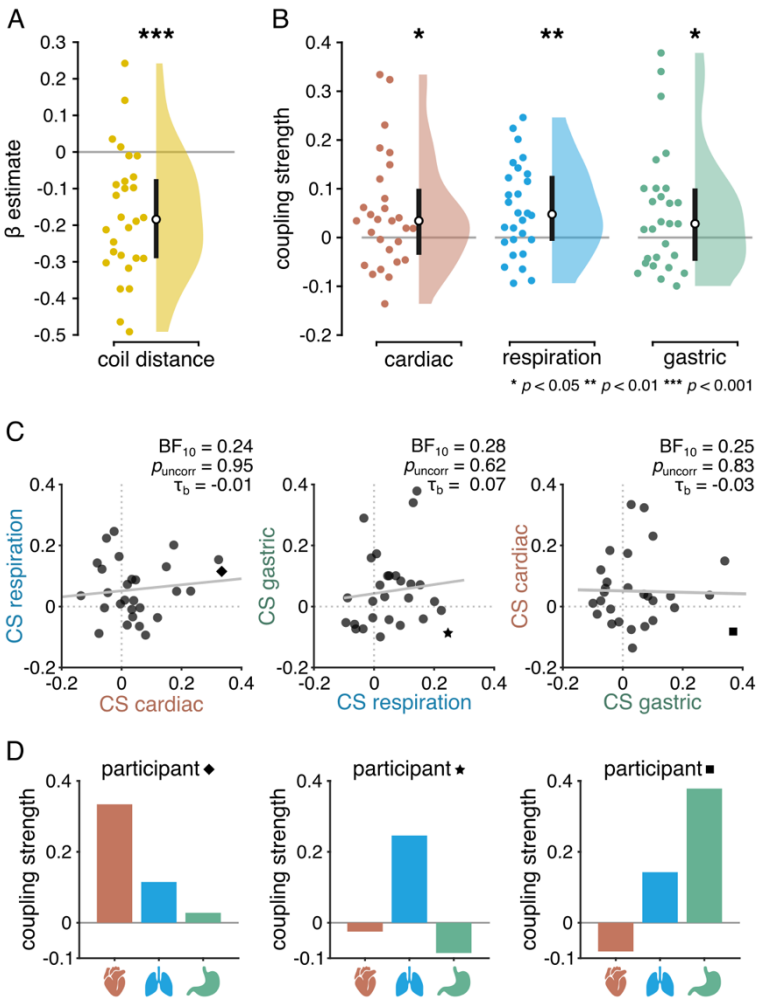

Figure 2. Sources of MEP amplitude fluctuations. A) The distance between the TMS coil and the cortical target in motor cortex significantly affect MEPs, with larger distances resulting in smaller MEPs. In all subsequent analyses, the influence of coil-to-target distance is regressed out from MEP amplitude. B) Coupling strengths (CS) between

each visceral rhythm and MEPs. CS reflects the difference between empirical and chance level coupling estimated with a circular GLM. Coupling strengths were significantly larger than zero for the cardiac, respiratory, and gastric rhythm. This means that the phase of the visceral rhythms impacted the amplitude of the MEP. C) Correlations between coupling strengths (CS) for each possible pair of visceral rhythm. There was moderate evidence for an absence of correlation between the coupling strengths of the different organs, showing that the phase-amplitude coupling between the viscera and motor system happened independent from one another. Note that for illustration purposes a regression line has been added to the figure, whereas the reported statistics are the result of a ranked correlation test (Kendall's tau). Notably in left panel the slope of the regression line is positive whereas the tau value is negative. D) Each participant displayed a unique interoceptive profile. To illustrate this inter-individual variability, interoceptive profile of the participant with the largest cardiac-motor coupling (left, lozenge in C), the largest respiration-motor coupling (middle, star in C), and the participant with the largest gastric-motor coupling (right, square in C). High coupling between corticospinal excitability and a given organ did not imply high coupling between corticospinal excitability and the two other organs investigated. * $p<0.05$; ** $p<0.01$; *** $p<0.001$

3.2 The amplitude of MEP varies with the phases of the three visceral rhythms

We first wanted to establish whether, as hypothesized, there was coupling between the phase of each of the visceral rhythms and the amplitude of the MEP. Phases are defined from R peak to R peak for the cardiac rhythm, from beginning of inspiration to end of expiration for the respiratory rhythm, and are unrelated to specific physiological events for the gastric rhythm, where such markers do not exist (33).

Using a circular spline GLM approach (39), we estimated, for each participant, how much MEP amplitude varies with the phase of each visceral rhythm. We computed coupling strengths, reflecting the difference between empirically obtained coupling scores and the median of chance level coupling scores obtained by permutation. We found coupling strengths to be significantly larger than zero for the cardiac (one -tailed Wilcoxon signed-rank test against zero, z = 1,79, p = 0.04, BF_{10} = 3.65, Hedge's g = 0.54), respiratory (z = 2.65p = 0.004, BF_{10} = 22.91, Hedge's g = 0.54), and gastric (z = 1.70, p = 0.04, BF_{10} = 2.85, Hedge's g = 0.49) rhythms (see figure 2B). This result demonstrates that fluctuations of corticospinal excitability over time are driven by the phase of each of the three visceral rhythms, with similar effect sizes at the group level.

3.3 Cardiac, respiratory, and gastric phase influences on corticospinal excitability vary independently from each other

At the participant's level, do we find evidence for interoceptive-sensitive or interoceptive-insensitive participants? In other words, is high coupling with one visceral rhythm predictive of high coupling with another visceral rhythm? We tested for this possibility by correlating the individual coupling strengths of the three visceral rhythms with each other (Figure 2C). We found no correlation between coupling strengths, with all tested correlations providing

moderate evidence for the null hypothesis (Kendall's tau B correlations, all *p* values > 0.62, all BF_{10} < 0.33). By exploring the interoceptive profiles of the participants with the highest coupling strength of each rhythm, it is apparent that high coupling with one rhythm does not necessarily mean high or even any coupling with another rhythm, and all types of interoceptive coupling profiles can be possible, as illustrated in figure 2D.

We confirmed those results using a second approach, where all rhythms were combined in the same general linear model. To switch from a circular spline model to a general linear model with interactions between rhythms, we defined for each participant and each rhythm an interval of pi where MEP amplitude was maximal (excitatory phase), and an interval of pi where MEP amplitude was minimal (inhibitory phase). For each participant, we then accounted for MEP amplitude by binarized phases for all three rhythms, and, importantly, all possible interactions between rhythms. The model confirms a significant influence of all three rhythms, as expected by the model design, but revealed an absence of interactions between rhythms: We found no double or triple interactions between any of the visceral phases (all *p* values for interaction terms > 0.18). Except for the interaction term between cardiac and gastric phases (BF_{10} = 0.47), all BF_{10} values indicate moderate evidence for the null hypothesis for all other interactions (BF_{10} < 0.33).

Together, these separate analyses show that even though the phase of each of the three visceral rhythms influences the amplitude of the MEP, they do so in an independent manner: at the participant's level, high coupling between motor excitability and one rhythm provides no information of the coupling with another rhythm, resulting in a large variety of individual interoceptive coupling profiles

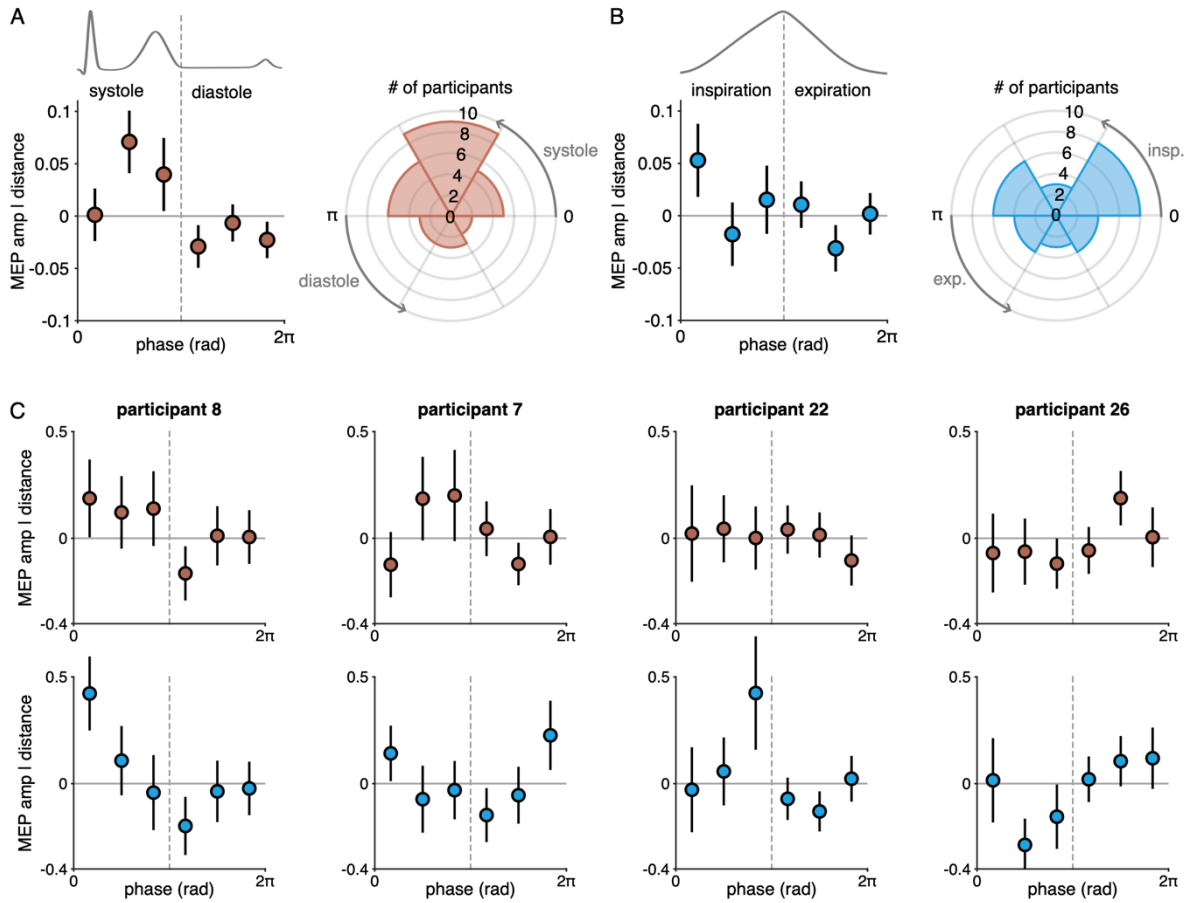

Figure 3. Absence of significant correlation between self-reported organ-specific interoception on the THISQ questionnaire and the respective coupling strength (CS) with corticospinal excitability of that organ, in the cardiac (left), respiratory (middle) and gastric (right) domains. Note that for illustration purposes a regression line has been added to the figure, whereas the reported statistics are the result of a ranked correlation test (Kendall's tau). Notably in right panel the slope of the regression line is positive whereas the tau value is negative.

3.4 Alignment to cardiac and respiratory phase shows inter-individual variability

The cardiac and respiratory rhythms can be subdivided in two meaningful physiological phases, respectively systole/diastole and inspiration/expiration. In an exploratory analysis, we find that in line with previous findings (23), at the group level, corticospinal excitability was enhanced in the systolic cardiac phase (figure 4A, left). In terms of variability, 20 out of 28 participants had their highest phase bin in the systolic phase (figure 4A, right), showing that most, but not all, participants followed the pattern for cardiac enhancement during systole. Regarding respiration, at the group level, corticospinal excitability was largest in early inspiration (figure 4B, left). This pattern is consistent with previously reported increased amplitudes of the readiness potential during inspiration (15), although the same study reported more action onsets during the end of expiration. Inter-subject variability appeared a bit larger

than for cardiac phase: 17 out of 28 participants had their maximal MEP amplitude during inspiration (figure 4B, right).

While group data suggest preferential phases of enhanced excitability, during cardiac systole and at the beginning of inspiration, there was also large inter-subject variability. We therefore further explored whether participants who deviated from the group pattern for cardiac phase also deviated from the group pattern for respiratory phase. As illustrated in Figure 4C, some participants followed the group pattern for both systole and inspiration (participant 8), others showed systolic coupling, but late expiration coupling (participant 7), some showed no coupling to the cardiac cycle, but an increased coupling during inspiration (participant 22), and lastly an example showing coupling to both rhythms, yet both divergent from the group pattern (participant 26).

This exploratory analysis thus reveals that although group level effects might indicate alignment to physiological phases of the cardiac and respiratory rhythms, some participants deviate from this alignment yet still display robust coupling with the corticospinal excitability.

3.5 No link between self-reported interoception and viscera-motor coupling

We then tested whether the strength of an individual's coupling between visceral phase and corticospinal excitability was related to how much an individual indicates to be aware of this specific organ. To this end, we correlated the coupling strength of each of the organs to the organ-specific scores of the recently developed THISQ questionnaire (34). There was no significant correlation between these two interoceptive measures (Kendall's tau B correlations; all $p > 0.10$). BF_{10} values indicate moderate evidence for the null hypothesis for the gastric data ($BF_{10} = 0.25$) and an undecided status for the cardiac and respiration data ($BF_{10} = 0.93$ and $BF_{10} = 0.47$ respectively, see figure 3). Note that for the cardiac and respiratory domains, if anything, the data would point to a negative correlation, whereas one could reasonably assume a priori a positive correlation. Altogether, the results indicate that whether a participant reports high subjective awareness of their heart, lungs, or stomach, is unrelated to the extent to which the organ's rhythm is coupled to motor cortex excitability.

Additionally, we tested whether viscera-motor coupling strengths were linked to a commonly used interoception questionnaire (MAIA-2 (35)) that mixes different organs into the same score or sub-score. We specifically focused on the sub-scores most related to awareness of internal sensations, body listening and noticing. Again, we find no significant correlations with either body listening (cardio $p_{FDR} = 0.30$, $\tau_b = 0.21$, $BF_{10} = 0.75$, respiration $p_{FDR} = 0.29$, $\tau_b = -0.27$,

BF_{10} = 1.74, gastric p_{FDR} = 0.89, τ_b = -0.02, BF_{10} = 0.25), or noticing (cardio p_{FDR} = 0.66, τ_b = -0.08, BF_{10} = 0.29, respiration p_{FDR} = 0.3, τ_b = -0.20, BF_{10} = 0.71, gastric p_{FDR} = 0.35, τ_b = -0.167, BF_{10} = 0.51).

Together, these results show that different questionnaires measuring the extent to which someone feels aware of their body, either in a precise organ-specific manner or more generally speaking, are unrelated to the extent to which there is motor-viscera coupling. Thus, self-reports and actual interoceptive coupling with motor excitability tap into different dimensions of interoception.

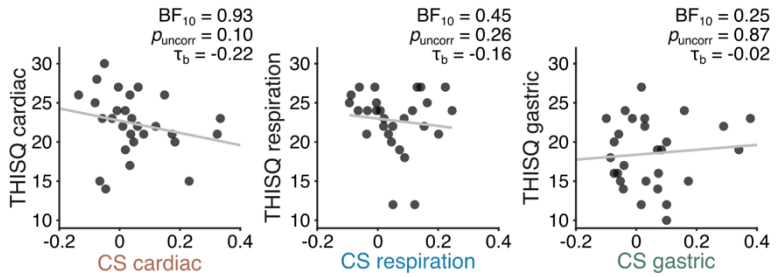

Figure 4. Exploratory analyses on alignment to cardiac systole/diastole and inspiration/expiration. A) Phase-binned mean MEP amplitudes, with 0 to π reflecting systole and π to 2 π diastole. At the group level, MEPs were larger in the systolic cardiac phase (left). The polar histogram (right) indicates the number of participants having their maximal coupling strengths in the bin. In 20 out of 28 participants, cardiac-motor excitability coupling peaked in systole. B) Phase-binned mean MEP amplitudes, with 0 to π reflecting inspiration and π to 2 π expiration. At the group level, MEPs were larger in the early inspiration phase (left), with 17/28 participants having their highest respiratory-motor excitability coupling during inspiration (right). C) Examples of individual data for cardiac (red) and respiratory (blue) coupling, revealing the extent of intersubject variability.

4. Discussion

To quantify organ-specificity in the coupling between interoceptive signals and the motor system, we tested whether the phase of the cardiac, respiratory, and gastric rhythm can explain fluctuations in corticospinal motor excitability. We demonstrate the existence of coupling between motor excitability and the cardiac, respiratory, and gastric rhythms, with similar effect sizes at the group level. We found significant coupling between motor excitability and each of the three rhythms, with similar effect sizes at the group level. However, this apparent similarity did not reflect a consistent pattern across individuals. Rather, participants who showed strong coupling with one rhythm did not necessarily show strong coupling with the others. This pattern of results indicates that the mechanisms underlying the coupling between motor excitability and the three visceral rhythms must be relatively independent from each other. The existence of coupling for all three rhythms despite very different physiological functions and time scales, and the independence of the coupling mechanisms, call for refining and specifying the functional interpretative frameworks on interoception. Intersubject variability was altogether large: not only participants displayed their own individual interoceptive profiles, but the preferred phase of cardiac or respiratory coupling could also vary. Finally, intersubject variability in viscera-motor coupling was not related to everyday life conscious interoceptive feelings as measured with questionnaires.

4.1 Independent influences of the three rhythms suggest at least partially distinct mechanisms

Our results show that motor excitability, measured from the hand region in primary motor cortex down to a specific muscle, is independently related to the cardiac, respiratory and gastric rhythms. Although one previous study revealed effects of cardiac phase on MEP amplitudes (23), null findings have also been reported (42–45). This discrepancy is likely explained by differences in the experimental design, such as TMS locking to fixed cardiac phases, which might miss the inter-individual variability in optimal phases demonstrated in this experiment, as well as fluctuations in TMS coil to cortical target distance, which was not considered in those studies. To the best of our knowledge, MEP amplitude fluctuations have never been reported along the respiratory or gastric rhythms – and in general, with few notable exceptions such as (15), the literature relating motor activity to interoception considers only one visceral rhythm at a time.

The independence of the effects suggests that each coupling is mediated by at least partially distinct mechanisms. Our results do not allow to be more specific about the nature of the mechanisms, but it is worth reminding that there are quite a number of possibilities. Firstly, while all three organs are connected to the central nervous systems through cranial nerves

and spino-thalamic pathways, there are also specificities. For instance, cardiac contractions translate into blood pulsations that might be directly transduced in the brain by both neurons and glial cells (46,47), and respiration is detected by olfactory receptors acting also as mechanoreceptors, inducing neural oscillations in large cortical territories (48–51). Because MEPs reflect a compound measure of cortical, spinal and muscle excitability, the effects could also partially be driven by peripheral interferences. In cats, motoneuron discharges have been shown to be modulated by both the cardiac cycle (22,52), as well as by respiratory phase (53–55), and arterial pulsations modulate muscle spindle discharge in humans (56). However, Transcranial Evoked Potentials, i.e. the cortical response to a TMS pulse measured with EEG that reflect cortical excitability only (57), differ in amplitude between cardiac systole and diastole (23). Therefore, at least the observed modulation of MEPs by the cardiac cycle in the current experiment might represent a mixture of alterations in both cortical and spinal excitability.

Finally, fluctuations in motor cortex excitability might arise from a modulation of the basal ganglia - motor loop. In mice, stimulation of gastric vagal afferents stimulates dopamine release in the nigro-striatal pathway (58). In humans, deep brain stimulation of the sub-thalamic nucleus in Parkinson patients (59) alleviates not only the motor, but also the gastric symptoms that commonly reported in this pathology (60). Collectively, those findings suggest that the basal ganglia – motor loop might be involved in the gastric-motor coupling we observe here – in other words, the coupling itself could begin outside primary motor cortex, but be revealed by TMS stimulation of the primary motor cortex.

4.2 Functional frameworks should be tightened and refined

We show that all three visceral rhythms independently contribute to motor excitability, which has implications for the functional frameworks that have been proposed to account for the coupling between visceral rhythms and the brain. The active sensing framework (6) is tightly linked to viscera-motor coupling. For example, in rodents respiratory phase is locked to onsets of whisker, nose, and head movements (61,62), which would form a strategic behavioural exploration state (63), and in humans, both visual (8) and tactile exploration (64) are dependent on the cardiac cycle. While the idea that there is a global bodily state, involving both visceral rhythms and motor readiness, favouring exploration is appealing, how could the three visceral rhythms play an independent role in modulating motor excitability in the active sensing framework? Clearly our data do not allow for a definite answer, and do not dismiss the active sensing framework. Rather, our results call for more specific predictions of the active sensing account, taking into account the existence of independent influences of each visceral rhythm on motor excitability.

Another prominent framework is the scaffolding hypothesis, which proposes that slower bodily rhythms can act as carrier frequencies for neural oscillations, thereby facilitating between-area communication. How could all three visceral rhythms independently fulfil this function? Different timescales of carrier waves could be matched to the temporal structure of incoming information (65), making it advantageous to have various bodily frequencies available. The different visceral rhythms might therefore serve different functions where coupling and decoupling occurs in a state-dependent manner – a proposal for which there is already some experimental evidence: the coupling between the respiratory rhythm and prefrontal cortex is specific to freezing states in mice (66), and there is more coupling of the brain to either the respiratory or the gastric rhythm in rest compared to cognitive tasks, during which temporal structures drastically change (67,68). As with the active sensing framework, the scaffolding hypothesis needs to be further defined to determine how multiple visceral rhythms could each subserve a function as carrier waves, potentially under different circumstances.

4.3 Variety of interoceptive profiles

The involvement of multiple mechanisms of coupling between visceral rhythms and motor excitability, acting with different weights in different participants, could account for the large inter-subject variability observed. Indeed, if at the group level the coupling with motor excitability was similar for all three rhythms, at the individual level all possible combinations of high/moderate/low coupling patterns were observed – for instance some participants showed large gastric coupling but only marginal respiratory and cardiac coupling, others showed moderate coupling with the three rhythms, etc. In other words, there were as many interoceptive profiles as there were participants. In addition, for the cardiac and respiratory rhythms, the largest motor excitability was most often found during cardiac systole and early inspiration, as would be expected from the literature (15,23), but a non-negligible proportion of participants displayed equally large coupling during diastole or during expiration. Considering the participant's preferred phase to alter viscero-motor coupling will prove important, both for studies aiming at dissecting mechanisms as well as clinical interventional studies. This sets a limit to the applicability of tasks and interventions in which stimuli are locked to fixed phases of visceral cycles.

Variability in interoceptive profiles was not explained by differences in interoceptive feelings as probed with questionnaire, also known as interoceptive sensitivity (69). This adds to growing evidence of a gap between objective and subjective measures of interoception (5,70). For instance, even when directly probed, participants reported no subjective awareness of the objectively measured coupling of motor actions and respiratory phase (15), and the ability at

detecting one's own heartbeats is unrelated to interoceptive self-reports (71–73). Such negative findings may have been partially driven by questionnaires conflating multiple viscera and fundamentally tapping into different constructs (74). To partly overcome this limitation, here correlations were calculated between organ-specific self-reports (34) and their respective organ-motor coupling score. Despite this, we still found an absence of correlation between self-reported interoception and objectively measured interoceptive influence on motor excitability. Whether and how objective and subjective measures of interoception relate to each other remains an open issue, with potential clinical relevance (3).

Lastly, interoception is often suspected to be impaired in psychiatric (see, e.g.(3)) as well as sometimes in neurological disorders (see, e.g., (60)) – but in practice in most cases only one aspect of interoception is probed : for instance, cardiac interoception is related to depression but not to anxiety (75,76). Our results on the variability in interoceptive profiles emphasize the need to test for more than one organ to explore the links between interoception and clinical features.

4.4 Conclusion

The coupling between the motor system and gastric, respiratory and cardiac rhythms can be measured by probing the cortico-spinal excitability of the hand. All three rhythms impact the motor control of the hand, they do so independently, and in different participants the influence of each rhythm is different. These findings have important consequences for how interoception is conceptualized: distinct mechanisms underly coupling between the visceral rhythms and the motor system. Our results call for further specification in frameworks mapping the functional role of coupling between visceral and neural rhythms: why and when does the brain couple to one or multiple of these rhythms and what functions does it serve? Going forward, multi-organ recordings combined with neuroimaging are needed to reveal the functional relevance of individual interoceptive profiles, with potential implications in the fields of psychiatry and neurology.

Acknowledgements

The authors thank Camille Straboni for her help in developing the respiration preprocessing pipeline. This work was funded by Agence Nationale pour la Recherche (ANR- 17-EURE-0017, ANR-10- IDEX-0001-02, ANR- 21-CE37-0031). CTB is supported by a senior fellowship of the Canadian Institute For Advanced Research (CIFAR) program in Brain, Mind and Consciousness. A CC-BY-NC public copyright license has been applied by the authors to the present document and will be applied to all subsequent versions up to the Author Accepted Manuscript arising from this submission, in accordance with the grant's open access conditions.

Data & code availability

The custom code and preprocessed data used for the analyses reported in this article are available through osf.io/6utgf/. Due to data protection regulations in the EU, individual anatomical MRI data cannot be made available online.

Credit authorship contribution statement

TE: conceptualization, methodology, formal analysis, investigation, data curation, writing original draft & editing, funding acquisition. TS & ATS: conceptualization, resources & writing – review & editing. CTB: conceptualization, methodology, formal analysis, writing original draft & editing, funding acquisition, supervision, project administration.

References

1. Sherrington CS. The Integrative Action of the Nervous System. Yale University Press; 1906. 37 p.
2. Khalsa SS, Adolphs R, Cameron OG, Critchley HD, Davenport PW, Feinstein JS, et al. Interoception and Mental Health: A Roadmap. Biol Psychiatry Cogn Neurosci Neuroimaging. 2018 Jun 1;3(6):501–13.
3. Nord CL, Garfinkel SN. Interoceptive pathways to understand and treat mental health conditions. Trends Cogn Sci. 2022 Jun 1;26(6):499–513.
4. Azzalini D, Rebollo I, Tallon-Baudry C. Visceral Signals Shape Brain Dynamics and Cognition. Trends Cogn Sci. 2019 Jun;23(6):488–509.
5. Engelen T, Solcà M, Tallon-Baudry C. Interoceptive rhythms in the brain. Nat Neurosci. 2023 Oct;26(10):1670–84.
6. Schroeder CE, Wilson DA, Radman T, Scharfman H, Lakatos P. Dynamics of Active Sensing and perceptual selection. Curr Opin Neurobiol. 2010 Apr 1;20(2):172–6.
7. Wachowiak M. All in a Sniff: Olfaction as a Model for Active Sensing. Neuron. 2011 Sep 22;71(6):962–73.
8. Galvez-Pol A, McConnell R, Kilner JM. Active sampling in visual search is coupled to the cardiac cycle. Cognition. 2020 Mar;196:104149.
9. Ohl S, Wohltat C, Kliegl R, Pollatos O, Engbert R. Microsaccades Are Coupled to Heartbeat. J Neurosci. 2016 Jan 27;36(4):1237–41.
10. Karalis N, Sirota A. Breathing coordinates cortico-hippocampal dynamics in mice during offline states. Nat Commun. 2022 Jan 24;13(1):467.
11. Tort ABL, Brankačk J, Draguhn A. Respiration-Entrained Brain Rhythms Are Global but Often Overlooked. Trends Neurosci. 2018 Apr 1;41(4):186–97.
12. Rebollo I, Tallon-Baudry C. The sensory and motor components of the cortical hierarchy are coupled to the rhythm of the stomach during rest. J Neurosci. 2022;42(11):2205–20.
13. Rebollo I, Devauchelle AD, Béranger B, Tallon-Baudry C. Stomach-brain synchrony reveals a novel, delayed-connectivity resting-state network in humans. Critchley H, editor. eLife. 2018 Mar 21;7:e33321.
14. Zaccaro A, Penna F della, Mussini E, Parrotta E, Perrucci MG, Costantini M, et al. Attention to cardiac sensations enhances the heartbeat-evoked potential during exhalation. iScience. 2024 Apr 19;27(4).
15. Park HD, Barnoud C, Trang H, Kannape OA, Schaller K, Blanke O. Breathing is coupled with voluntary action and the cortical readiness potential. Nat Commun. 2020 Dec;11(1):289.
16. Waselius T, Xu W, Sparre JI, Penttonen M, Nokia MS. Cardiac cycle and respiration phase affect responses to the conditioned stimulus in young adults trained in trace eyeblink conditioning. J Neurophysiol. 2022 Mar;127(3):767–75.
17. Konttinen N, Mets T, Lyytinen H, Paananen M. Timing of Triggering in Relation to the Cardiac Cycle in Nonelite Rifle Shooters. Res Q Exerc Sport. 2003 Dec 1;
18. Kunzendorf S, Klotzsche F, Akbal M, Villringer A, Ohl S, Gaebler M. Active information sampling varies across the cardiac cycle. Psychophysiology. 2019 May;56(5):e13322.
19. Palser ER, Glass J, Fotopoulou A, Kilner JM. Relationship between cardiac cycle and the timing of actions during action execution and observation. Cognition. 2021 Dec 1;217:104907.
20. Rae CL, Botan VE, Gould van Praag CD, Herman AM, Nyyssönen JAK, Watson DR, et al. Response inhibition on the stop signal task improves during cardiac contraction. Sci Rep. 2018 Jun 14;8(1):9136.
21. Marshall AC, Ren Q, Enk L, Liu J, Schütz-Bosbach S. The effect of cardiac phase on distractor suppression and motor inhibition in a stop-signal task. Sci Rep. 2024 Dec 2;14(1):29847.
22. Ford TW, Kirkwood PA. Cardiac modulation of alpha motoneuron discharges. J Neurophysiol. 2018 May;119(5):1723–30.

23. Al E, Stephani T, Engelhardt M, Haegens S, Villringer A, Nikulin VV. Cardiac activity impacts cortical motor excitability. PLOS Biol. 2023 Nov 28;21(11):e3002393.
24. Johannknecht M, Kayser C. The influence of the respiratory cycle on reaction times in sensory-cognitive paradigms. Sci Rep. 2022 Feb 16;12(1):2586.
25. Schulz A, Schilling TM, Vögele C, Larra MF, Schächinger H. Respiratory modulation of startle eye blink: a new approach to assess afferent signals from the respiratory system. Philos Trans R Soc B Biol Sci. 2016 Nov 19;371(1708):20160019.
26. Kluger DS, Gross J. Depth and phase of respiration modulate cortico-muscular communication. NeuroImage. 2020 Nov 15;222:117272.
27. Li S, Rymer WZ. Voluntary Breathing Influences Corticospinal Excitability of Nonrespiratory Finger Muscles. J Neurophysiol. 2011 Feb;105(2):512–21.
28. Shirakawa K, Yunoki T, Afroundeh R, Lian CS, Matsuura R, Ohtsuka Y, et al. Voluntary breathing increases corticospinal excitability of lower limb muscle during isometric contraction. Respir Physiol Neurobiol. 2015 Oct 1;217:40–5.
29. Cao J, Lu KH, Oleson ST, Phillips RJ, Jaffey D, Hendren CL, et al. Gastric stimulation drives fast BOLD responses of neural origin. NeuroImage. 2019 Aug 15;197:200–11.
30. Cao J, Wang X, Chen J, Zhang N, Liu Z. The vagus nerve mediates the stomach-brain coherence in rats. NeuroImage. 2022 Nov 1;263:119628.
31. Bestmann S, Krakauer JW. The uses and interpretations of the motor-evoked potential for understanding behaviour. Exp Brain Res. 2015 Mar;233(3):679–89.
32. Spampinato DA, Ibanez J, Rocchi L, Rothwell J. Motor potentials evoked by transcranial magnetic stimulation: interpreting a simple measure of a complex system. J Physiol. 2023;601(14):2827–51.
33. Wolpert N, Rebollo I, Tallon-Baudry C. Electrogastrography for psychophysiological research: Practical considerations, analysis pipeline, and normative data in a large sample. Psychophysiology. 2020 Sep;57(9).
34. Vlemincx E, Walentynowicz M, Zamariola G, Van Oudenhove L, Luminet O. A novel self-report scale of interoception: the three-domain interoceptive sensations questionnaire (THISQ). Psychol Health. 2023 Sep 2;38(9):1234–53.
35. Mehling WE, Acree M, Stewart A, Silas J, Jones A. The Multidimensional Assessment of Interoceptive Awareness, Version 2 (MAIA-2). PLOS ONE. 2018 Dec 4;13(12):e0208034.
36. Oostenveld R, Fries P, Maris E, Schoffelen JM. FieldTrip: Open Source Software for Advanced Analysis of MEG, EEG, and Invasive Electrophysiological Data. Comput Intell Neurosci. 2011;2011:1–9.
37. Vázquez-Seisdedos CR, Neto JE, Marañón Reyes EJ, Klautau A, Limão de Oliveira RC. New approach for T-wave end detection on electrocardiogram: Performance in noisy conditions. Biomed Eng OnLine. 2011 Sep 9;10(1):77.
38. Liang F, Paulo R, Molina G, Clyde MA, Berger JO. Mixtures of g Priors for Bayesian Variable Selection. J Am Stat Assoc. 2008 Mar 1;103(481):410–23.
39. Kramer MA, Eden UT. Assessment of cross-frequency coupling with confidence using generalized linear models. J Neurosci Methods. 2013 Oct 30;220(1):64–74.
40. Claudino L, Hussain SJ, Buch ER, Cohen LG. Offline coil position denoising enhances detection of TMS effects. bioRxiv; 2018.
41. Numssen O, Martin S, Williams K, Knösche TR, Hartwigsen G. Quantification of subject motion during TMS via pulsewise coil displacement. Brain Stimulat. 2024 Sep 1;17(5):1045–7.
42. Bianchini E, Mancuso M, Zampogna A, Guerra A, Suppa A. Cardiac cycle does not affect motor evoked potential variability: A real-time EKG-EMG study. Brain Stimulat. 2021 Jan;14(1):170–2.
43. Filippi MM, Oliveri M, Vernieri F, Pasqualetti P, Rossini PM. Are autonomic signals influencing cortico-spinal motor excitability?: A study with transcranial magnetic stimulation. Brain Res. 2000 Oct 27;881(2):159–64.
44. Otsuru N, Miyaguchi S, Kojima S, Yamashiro K, Sato D, Yokota H, et al. Timing of Modulation of Corticospinal Excitability by Heartbeat Differs with Interoceptive Accuracy. Neuroscience. 2020 May;433:156–62.

45. Paci M, Cardellicchio P, Di Luzio P, Perrucci MG, Ferri F, Costantini M. When the heart inhibits the brain: Cardiac phases modulate short-interval intracortical inhibition. iScience. 2024 Mar;27(3):109140.
46. Jammal Salameh L, Bitzenhofer SH, Hanganu-Opatz IL, Dutschmann M, Egger V. Blood pressure pulsations modulate central neuronal activity via mechanosensitive ion channels. Science. 2024 Feb 2;383(6682):eadk8511.
47. Kim KJ, Diaz JR, Iddings JA, Filosa JA. Vasculo-Neuronal Coupling: Retrograde Vascular Communication to Brain Neurons. J Neurosci. 2016 Dec 14;36(50):12624–39.
48. Gonzalez J, Torterolo P, Tort AB. Mechanisms and functions of respiration-driven gamma oscillations in the primary olfactory cortex. Colgin LL, editor. eLife. 2023 Feb 20;12:e83044.
49. González J, Cavelli M, Mondino A, Castro-Zaballa S, Brankačk J, Draguhn A, et al. Breathing modulates gamma synchronization across species. Pflugers Arch. 2023 Jan;475(1):49–63.
50. Tort ABL, Komorowski R, Eichenbaum H, Kopell N. Measuring Phase-Amplitude Coupling Between Neuronal Oscillations of Different Frequencies. J Neurophysiol. 2010 Aug;104(2):1195–210.
51. Zhuang L, Zhang B, Qin Z, Wang P. Nasal Respiration is Necessary for the Generation of γ Oscillation in the Olfactory Bulb. Neuroscience. 2019 Feb 1;398:218–30.
52. Kirkwood PA, Romaniuk JR, Kowalski KE. Further observations on cardiac modulation of thoracic motoneuron discharges. Neurosci Lett. 2019 Feb 16;694:57–63.
53. Ford TW, Kirkwood PA. Respiratory drive in hindlimb motoneurones of the anaesthetized female cat. Brain Res Bull. 2006 Oct 16;70(4):450–6.
54. Kirkwood PA, Lawton M, Ford TW. Plateau potentials in hindlimb motoneurones of female cats under anaesthesia. Exp Brain Res. 2002 Oct 1;146(3):399–403.
55. Enríquez Denton M, Wienecke J, Zhang M, Hultborn H, Kirkwood PA. Voltage-dependent amplification of synaptic inputs in respiratory motoneurones. J Physiol. 2012;590(13):3067–90.
56. Birznieks I, Boonstra TW, Macefield VG. Modulation of Human Muscle Spindle Discharge by Arterial Pulsations - Functional Effects and Consequences. PLOS ONE. 2012 Apr 17;7(4):e35091.
57. Hernandez-Pavon JC, Veniero D, Bergmann TO, Belardinelli P, Bortoletto M, Casarotto S, et al. TMS combined with EEG: Recommendations and open issues for data collection and analysis. Brain Stimul Basic Transl Clin Res Neuromodulation. 2023 Mar 1;16(2):567–93.
58. Han W, Tellez LA, Perkins MH, Perez IO, Qu T, Ferreira J, et al. A Neural Circuit for Gut-Induced Reward. Cell. 2018 Oct 18;175(3):665-678.e23.
59. Krygowska-Wajs A, Furgala A, Gorecka-Mazur A, Pietraszko W, Thor P, Potasz-Kulikowska K, et al. The effect of subthalamic deep brain stimulation on gastric motility in Parkinson's disease. Parkinsonism Relat Disord. 2016 May 1;26:35–40.
60. Araki N, Yamanaka Y, Poudel A, Fujinuma Y, Katagiri A, Kuwabara S, et al. Electrogastrography for diagnosis of early-stage Parkinson's disease. Parkinsonism Relat Disord. 2021 May 1;86:61–6.
61. Kleinfeld D, Deschênes M, Economo MN, Elbaz M, Golomb D, Liao SM, et al. Low- and high-level coordination of orofacial motor actions. Curr Opin Neurobiol. 2023 Dec 1;83:102784.
62. Kurnikova A, Moore JD, Liao SM, Deschênes M, Kleinfeld D. Coordination of Orofacial Motor Actions into Exploratory Behavior by Rat. Curr Biol. 2017 Mar 6;27(5):688–96.
63. Findley TM, Wyrick DG, Cramer JL, Brown MA, Holcomb B, Attey R, et al. Sniff-synchronized, gradient-guided olfactory search by freely moving mice. Bhalla US, Dulac C, editors. eLife. 2021 May 4;10:e58523.
64. Galvez-Pol A, Virdee P, Villacampa J, Kilner J. Active tactile discrimination is coupled with and modulated by the cardiac cycle. Pruszynski JA, de Lange FP, Holmes N, Allen M, editors. eLife. 2022 Oct 12;11:e78126.

65. Lakatos P, Gross J, Thut G. A New Unifying Account of the Roles of Neuronal Entrainment. Curr Biol. 2019 Sep 23;29(18):R890–905.
66. Bagur S, Lefort JM, Lacroix MM, de Lavilléon G, Herry C, Chouvaeff M, et al. Breathing-driven prefrontal oscillations regulate maintenance of conditioned-fear evoked freezing independently of initiation. Nat Commun. 2021 May 10;12(1):2605.
67. Balasubramani PP, Walke A, Grennan G, Perley A, Purpura S, Ramanathan D, et al. Simultaneous Gut-Brain Electrophysiology Shows Cognition and Satiety Specific Coupling. Sensors. 2022 Jan;22(23):9242.
68. Kluger DS, Gross J, Keitel C. A Dynamic Link between Respiration and Arousal. J Neurosci. 2024 Nov 20;44(47).
69. Garfinkel SN, Seth AK, Barrett AB, Suzuki K, Critchley HD. Knowing your own heart: Distinguishing interoceptive accuracy from interoceptive awareness. Biol Psychol. 2015 Jan 1;104:65–74.
70. Suksasilp C, Garfinkel SN. Towards a comprehensive assessment of interoception in a multi-dimensional framework. Biol Psychol. 2022 Feb 1;168:108262.
71. Calì G, Ambrosini E, Picconi L, Mehling W, Committeri G. Investigating the relationship between interoceptive accuracy, interoceptive awareness, and emotional susceptibility. Front Psychol. 2015 Aug 24;6.
72. Critchley HD, Wiens S, Rotshtein P, Öhman A, Dolan RJ. Neural systems supporting interoceptive awareness. Nat Neurosci. 2004 Feb;7(2):189–95.
73. Ferentzi E, Drew R, Tihanyi BT, Köteles F. Interoceptive accuracy and body awareness – Temporal and longitudinal associations in a non-clinical sample. Physiol Behav. 2018 Feb 1;184:100–7.
74. Desmedt O, Heeren A, Corneille O, Luminet O. What do measures of self-report interoception measure? Insights from a systematic review, latent factor analysis, and network approach. Biol Psychol. 2022 Mar 1;169:108289.
75. Adams KL, Edwards A, Peart C, Ellett L, Mendes I, Bird G, et al. The association between anxiety and cardiac interoceptive accuracy: A systematic review and meta-analysis. Neurosci Biobehav Rev. 2022 Sep;140(104754).
76. Qi M, Shen X, Zeng Y, Lin X, Suliman M, Li P. Interoception and mental health in middle-aged and elderly adults: A systematic review and meta-analysis. Neurosci Biobehav Rev. 2025 May;172:106104.

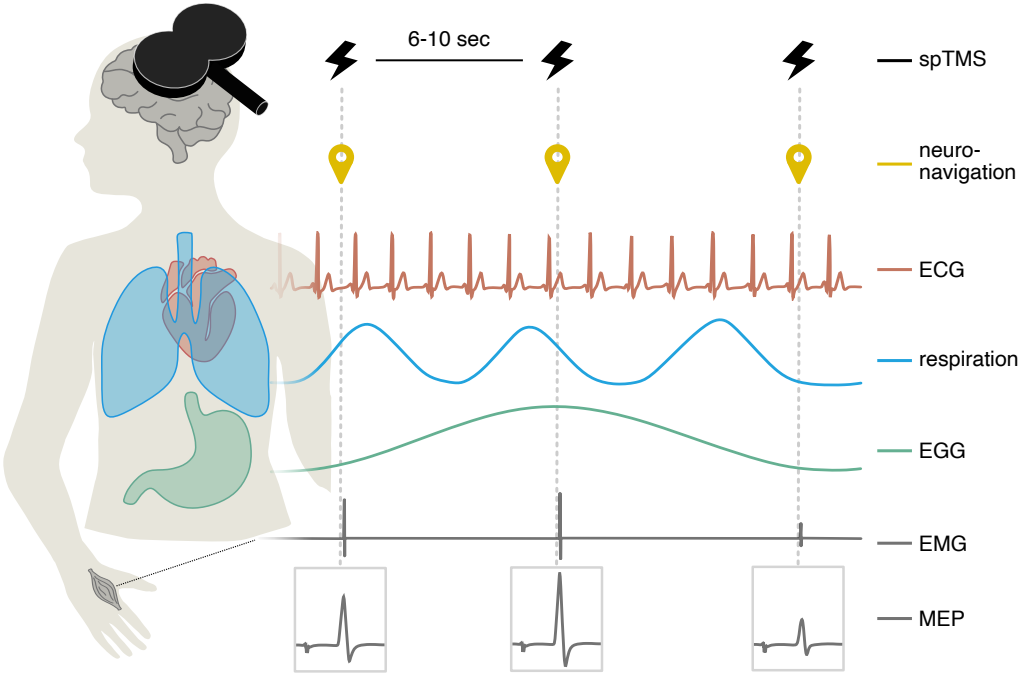
6-10 sec
spTMS
neuro-
navigation
ECG
respiration
EGG
EMG
MEP

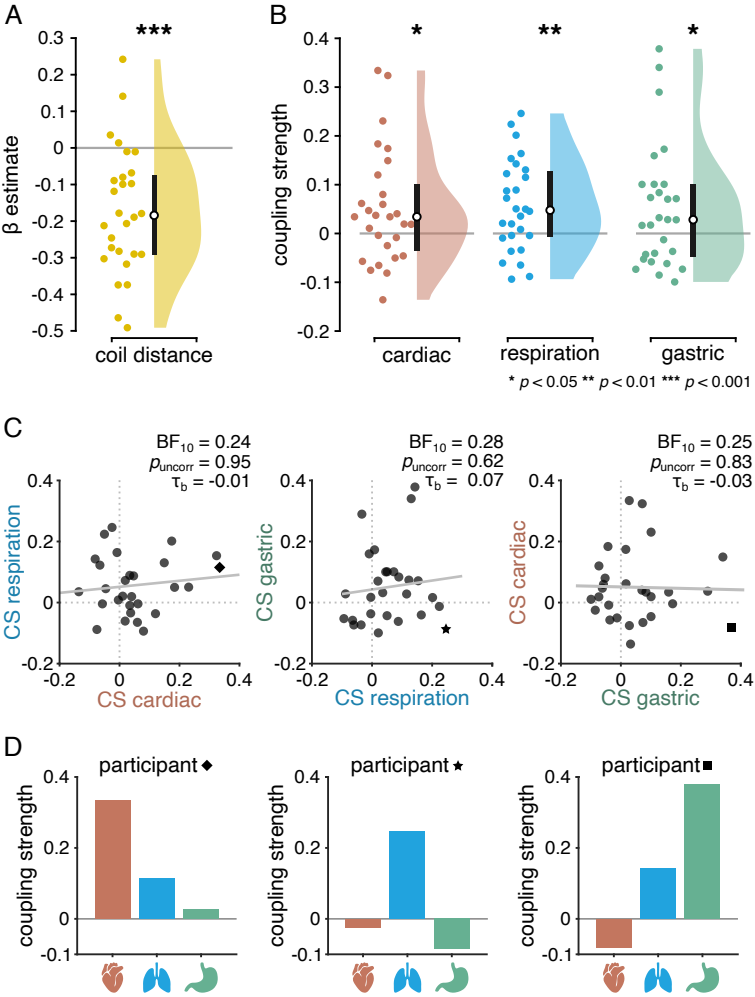
A
***
β estimate
0.3
0.2
0.1
0
-0.1
-0.2
-0.3
-0.4
-0.5
coil distance
B
*
**
*
coupling strength
0.4
0.3
0.2
0.1
0
-0.1
-0.2
cardiac
respiration
gastric
* p < 0.05 ** p < 0.01 *** p < 0.001
C
BF10 = 0.24
puncorr = 0.95
τb = -0.01
CS respiration
CS cardiac
BF10 = 0.28
puncorr = 0.62
τb = 0.07
CS gastric
CS respiration
BF10 = 0.25
puncorr = 0.83
τb = -0.03
CS cardiac
CS gastric
0.4
0.2
0
-0.2
-0.2
0
0.2
0.4
D
participant ◆
participant ★
participant ■
coupling strength
0.4
0.2
0
-0.1

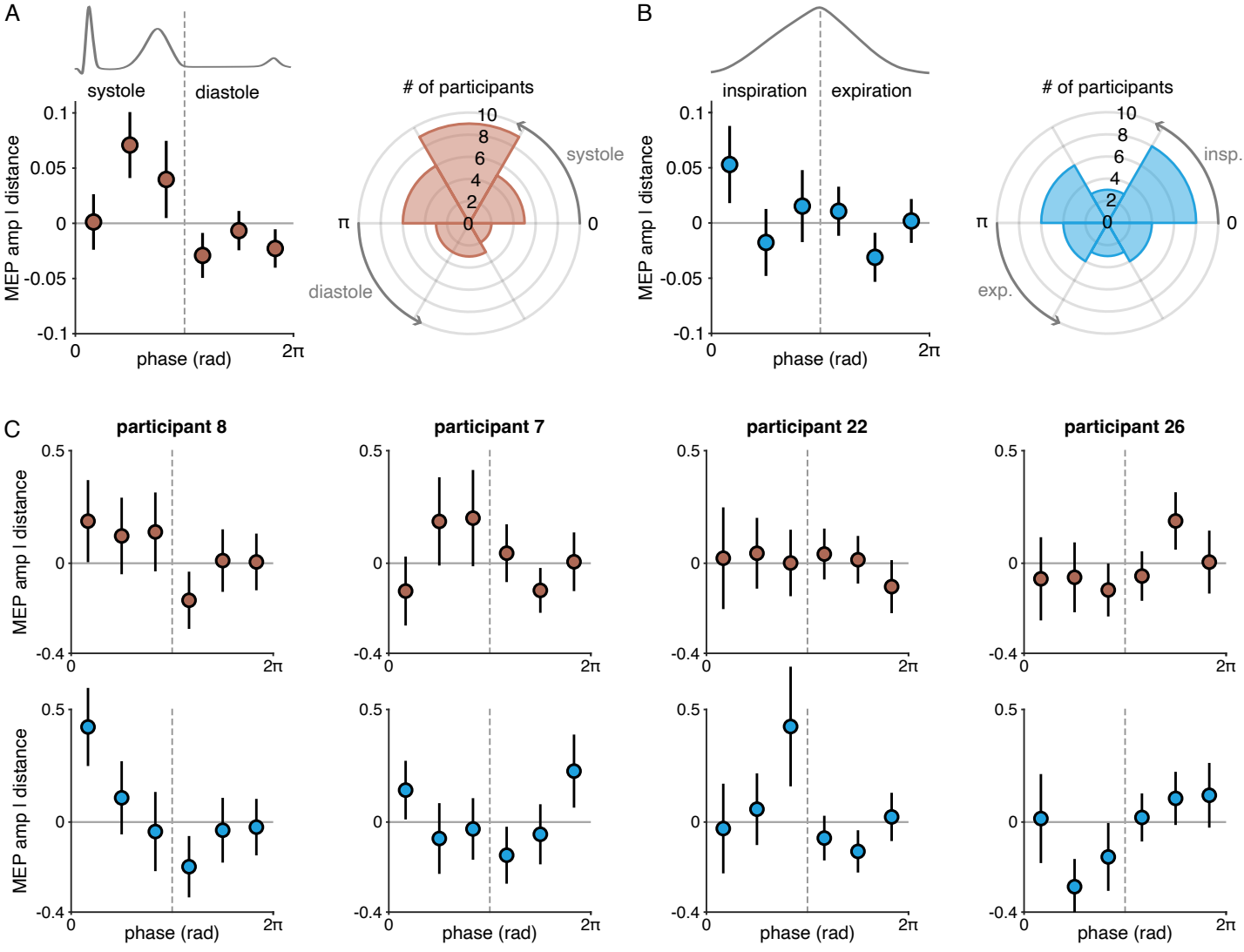
A
systole
diastole
MEP amp I distance
phase (rad)
# of participants
systole
diastole
B
inspiration
expiration
MEP amp I distance
phase (rad)
# of participants
insp.
exp.
C
participant 8
participant 7
participant 22
participant 26
MEP amp I distance
phase (rad)

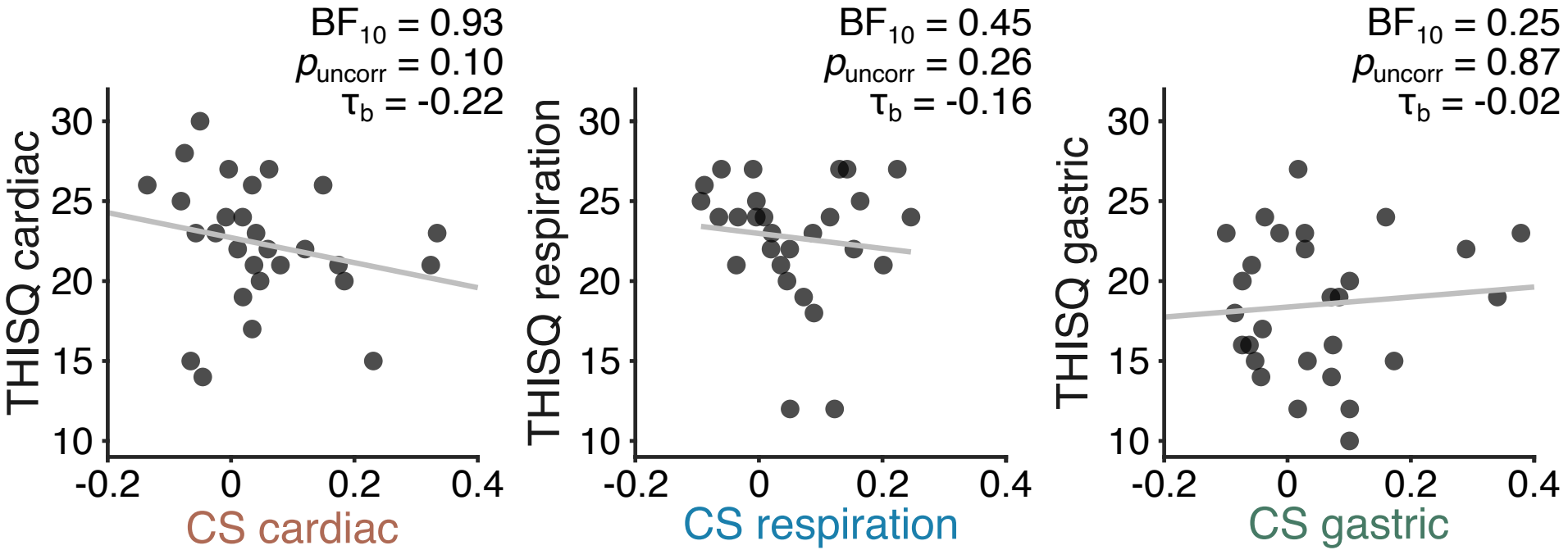
BF10 = 0.93
puncorr = 0.10
τb = -0.22
THISQ cardiac
CS cardiac
BF10 = 0.45
puncorr = 0.26
τb = -0.16
THISQ respiration
CS respiration
BF10 = 0.25
puncorr = 0.87
τb = -0.02
THISQ gastric
CS gastric
30
25
20
15
10
-0.2
0
0.2
0.4